

The Influence of Fabrication Process on the Initial Stages of Steam Oxidation Performed on Haynes[®] 282[®] Alloy at 760 °C

T. Dudziak, L. Boron, M. Homa, R. Nowak, N. Horton, R. Sheppard, R.M. Purgert, A. Siewiorek, N. Sobczak, and J.J. Sobczak

(Submitted August 4, 2016; in revised form October 3, 2016; published online November 11, 2016)

This work presents results observed after the first 5 h of oxidation of Haynes[®] 282[®] alloy. The steam oxidation tests have been carried out in pure water at 760 °C for 1, 2 and 5 h, respectively, using an accurate thermogravimetric balance technique. The alloy used for comparison in this work was fabricated using three different methods. The initial steam oxidation performance of the commercially wrought alloy Haynes[®] 282[®] was compared with a fabricated cast alloy and a HIP/PM alloy. The results show that in terms of corrosion resistance, fabrication techniques appear to have little impact on steam oxidation performance and behavior. The exposed Ni-based alloys all developed the oxide scales consisting mainly of Cr₂O₃ phase mixed with some TiO₂, while internal Al and Ti precipitations along the grain boundaries were observed both in Haynes[®] 282[®] wrought and HIP/PM alloy.

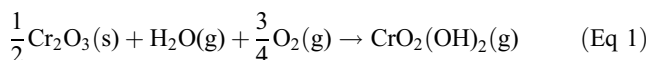
Keywords Haynes[®] 282[®], Ni-based superalloy, steam oxidation, TGA

1. Introduction

Raising environmental awareness is driving the global economy toward the reduction of CO₂ emissions and fuel consumption (Ref 1). The Energy sector is contributing to these goals by increasing power generation efficiency, which, for conventional systems, is a strong function of temperature coupled with the pressure of steam entering the turbine (Ref 2–4). Higher operational temperatures, however, can cause serious problems for boiler components in the steam turbine, not the least of which is reduced component lifetime. Thus, steam oxidation of high-temperature-resistant alloys has an important impact on power plant lifetime and overall operating efficiency. Higher operating temperatures significantly accelerate oxidation processes, which in turn leads to the development of thick, non-protective oxide scales, especially in low-alloyed ferritic steel types such as T22 and 16Mo3. The important concern resulting from fast oxide growth is a reduction of heat transfer and reduced ability to withstand high steam pressures due to high metal loss (Ref 5). Moreover, the stresses generated during the oxide growth change the scale morphology, leading to exfoliation and eventual material failure and/or tube or pipe blockage (Ref 6). Therefore, understanding steam oxidation processes and factors influencing them is crucial for improving

power plant efficiency (Ref 7). Currently, the research for crucial power plant components focuses on understanding steam oxidation behavior at steam temperatures up to 650, 700 and 760 °C for European COST522, European Thermie and US Department of Energy's Ultra Super Critical (USC) and Advanced Ultra Super Critical (A-USC) programs, respectively. In particular, to achieve required temperatures for USC and A-USC, Ni-based alloys with adequate mechanical properties and steam oxidation resistance are primarily considered the best candidate materials for the hottest areas of coal fired power plants such as super heaters (SH) and reheaters (RH).

Nevertheless, Ni-based alloys under long-term exposures at high temperatures (> 650 °C) may undergo chromia volatilization phenomena from the Cr₂O₃-rich scale, leading to catastrophic corrosion degradation (Ref 8). The process can be illustrated by the following reaction (Ref 9):



The volatilization of chromia scales leads to chromium depletion from the oxide scale and breakdown of the protective Cr₂O₃ scale, and increases the oxidation rate due to the nucleation of fast growing Ni-rich oxide and Fe-rich oxide when the rich Cr steels are exposed.

The formation of rich, stable, long-lasting Cr₂O₃ scale is essential for high performance of Ni-based alloys in USC or A-USC conditions (Ref 9). The scales formed on Ni-based alloys with Cr content higher than 16 wt.% are described as very thin and hard to observe (Ref 10). The scale consists of Cr₂O₃ with the addition of MnCr₂O₄ and some traces of γ(Ni). The studies performed on Haynes[®] 230[®] and Haynes[®] 282[®] Ni-based alloys at 760 °C in 10% water vapor and air-containing environments by Deodeshmukh (Ref 11) showed that the surface on Haynes[®] 230[®] was covered mainly by Cr₂O₃. In the case of the Haynes[®] 282[®] alloy, the scale was TiO₂ enriched along with Cr₂O₃. According to work carried out by Wright et al. (Ref 12), long exposure at 800 °C of Ni-based alloys Inconel 617 and Haynes[®] 230[®] showed that the oxide scale consists mainly of Cr₂O₃; however, the alloys underwent

T. Dudziak, L. Boron, M. Homa, R. Nowak, A. Siewiorek, N. Sobczak, and J.J. Sobczak, Centre for High Temperature Studies, Foundry Research Institute, 73 Zakopianska St., 30-418 Kraków, Poland; and N. Horton, R. Sheppard, and R.M. Purgert, Energy Industries of Ohio, Park Centre Plaza, Suite 200, 6100 Oak Tree Boulevard, Independence, OH 44131. Contact e-mail: tomasz.dudziak@iod.krakow.pl.

degradation due to an internal oxidation process, with the Inconel 617 showing a much higher degree of internal precipitates than that observed in Haynes[®] 230[®].

To date, the majority of studies in scientific literature are concerned with long-term exposures of Ni-based alloys (Ref 10, 12) at high temperature; however, in this work Haynes[®] 282[®] Ni-based alloys were exposed to very short intervals at 760 °C to investigate characteristics during the first hours of the oxidation process in pure water steam. The tests were conducted to evaluate corrosion by-products developed on the exposed surfaces. Generally, corrosion resistance of the exposed alloy over a prolonged term is primarily a function of effects occurring during the initial stage of oxidation. Cr₂O₃ and Al₂O₃ are well-known oxides delivering a high rate of protection at high temperature; however there are little published data on the initial stages of oxidation in Ni-based alloys. Thermodynamic properties of both Cr and Al strongly influence the initial behavior of Ni-based alloys, thus demonstrating the potential advantages of alloying elements such as Ni-Cr-Al. The ratio between Cr and Al plays an important role in the initial stage of oxidation on the Ni-based alloy, including its ability to form a protective scale. Furthermore, the relationship between Al and Cr reactivity highly influences the behavior of the Ni-based alloy when it is exposed to high temperature. Moreover, the potential effect of differing manufacturing methods on the first stages of high-temperature steam oxidation behavior of the Haynes[®] 282[®] was examined as well, to evaluate changes in chemical composition of the oxide scales between three different Haynes[®] 282[®] alloys. Commercially wrought alloy Haynes[®] 282[®] was compared with the same alloy after its melting and casting (H282-cast) and after sintering (H282-sint) from atomized powder using the HIP/PM process (Hot Isostatic Pressing/Powder Metallurgy). The post-exposed samples were investigated using standard analytical techniques.

2. Materials

In this work, samples of the same alloy, fabricated according to the three different methods set forth below, were tested:

1. Commercially available wrought Haynes[®] 282[®] alloy rods produced by Haynes International (USA);
2. As-cast alloy (H282-cast) produced at the Foundry Research Institute (Krakow, Poland) by melting wrought Haynes[®] 282[®] alloy rods in atmospheric air in a medium-frequency furnace using 40 kg crucible capacity lined with alumina. During heating and melting, the alloy surface was covered with argon and deoxidized with a nickel-magnesium master alloy. The molten alloy was then poured under gravity at 1560 °C into a phenol-formaldehyde resin sand coated with zirconia-based binder (Ref 13). The alloy cooled down to room temperature without any force conditions.
3. HIP/PM powder (H282-sint) was made by Carpenter Powder Products Inc. (USA) in cooperation with Energy Industry of Ohio (USA) using argon gas atomization that produced powder from the wrought alloy using the Micro-Melt[®] process. This screened powder was then compacted under high neutral gas (argon) isostatic pressure at elevated temperature to form the test pieces (Ref 14).

The chemical composition by weight percentage (wt.%) of the powder used to produce the H-282 alloy has the following composition: Ni: 57, Cr: 20, Co: 10, Mo: 8.5, Ti: 2.1, Al: 1.5, Fe: 0.3, Si: 0.15, C: 0.06 and B: 0.005. The raw powder was screened to a -60 mesh, yielding a maximum particle size diameter of $\leq \sim 250 \mu\text{m}$ including fines. The alloy H282-sint was manufactured using Hot Isostatic Pressure (HIP) technology at $1162.8 \pm 3 \text{ }^\circ\text{C}$ for $240 \pm 15 \text{ min}$ under pressure reaching 101.7 bar. The whole process was conducted under high-purity Ar gas in order to eliminate oxidation process during HIP procedure.

The alloy was heat-treated under a three-stage process. In Stage 1, the alloy was solution-annealed at 1121-1149 °C, for 12 h then gas-fan-cooled (GFC). In Stage 2, the alloy was precipitation age-hardened at 1010 °C for 2 h and then air-cooled. In Stage 3, the alloy was reheated to 788 °C and held for 16 h and then air-cooled (Ref 15).

Prior to the high-temperature tests, the samples with a $10 \times 10 \times 2 \text{ mm}$ dimension were ultrasonically cleaned for 15 minutes at 40 °C. Initial weights were accurately measured using a digital scale with accuracy of 0.001 mg.

3. Experimental Procedure

Steam oxidation experiments were performed using a thermogravimetric balance device (NETZSCH STA 449 F3 Jupiter), equipped with a residual gas analyzer QMS 403C Aëolos. The work was carried out within the DIN 51006 Thermal Analysis (TA); Thermogravimetry (TG) standard. In the study, nine squared samples were used. The samples were exposed for 1, 2 and 5 h, respectively, using heat-up and cool-down rates set at 10 °C/min. To ensure accuracy, prior to each test, the thermogravimetric scale with accuracy of 0.025 μg was set up to calibrate all parameters using a self-testing function. A humidity generator was used in the NETZSCH instruments to carry out measurements under humid atmospheres, i.e., steam oxidation.

In this work, deionized water from the tank located underneath the thermogravimetric balance was transported throughout the heating transfer line. The heating transfer line with maximum operating temperatures of 200 °C was set up for 180 °C. The purging synthetic gas containing 80% vol. nitrogen and 20% vol. oxygen was initially connected to the system and run for 2 h with the recommended 50 ml/min flow in order to clean the furnace of moisture and impurities. Further, during the tests, a protective gas (Ar) was used with 50 ml/min flow rate. The purge gas and protective gas were not delivered and were not mixed with steam in the furnace; rather, both gases were used only to clean and protect the balance underneath the steam furnace, ensuring the tests were performed in pure steam conditions. The test temperature was designed for 760 °C.

The post-process deionized water was returned to the condenser to close the cycle. During high-temperature tests, weight changes (mg) of the exposed sample against time (h) were plotted automatically. Prior to the steam oxidation experiments, the chemistry of the samples was characterized using energy-dispersive x-ray spectrometry (EDS). The outcomes of the measurements are shown in Table 1. The

Table 1 Chemical composition measured in wt.% by EDS on the samples prior to steam oxidation tests

Composition by EDS in FRI	Material	Elements, wt. %										
		C	Ni	Cr	Co	Mo	Ti	Al	Fe(a)	Mn	Si	B(b)
	H282-cast	0.1	Bal.	18.3	10.0	8.2	2.1	1.9	0.3	0.3	0.17	...
	H282-sint	0.1	Bal.	19.0	10.7	7.7	2.5	1.5	0.7	0.3	0.19	...
	Wrought Haynes [®] 282 [®]	0.1	Bal.	20.0	10.2	8.5	2.1	1.5	1.5	0.3	0.15	0.005

(a) Maximum. (b) Undetectable

analytical investigations were compared with the nominal composition provided by Haynes International (Ref 16).

4. Results

4.1 Kinetics

Figure 1(a), (b) and (c) shows the changes in mass (mg/cm²) versus time (h) for all the samples exposed in the study. It was found that the highest mass gain was achieved for the oxidized H282-cast alloy, whereas the oxidized H282-sint showed the lowest values after 1, 2 and 5 h of exposure, respectively. Moderate mass gain was achieved in the commercially available wrought Haynes[®] 282[®] alloy. The changes were observed in all three materials used in this work; thus, it can be concluded that the fabrication technique does have an impact on the mass gain during the steam oxidation process. Of the three samples, the H282-cast material indicated the lowest mass gain after 1 h of oxidation and remained lowest as the test continued for 2 h, while values between Haynes[®] 282[®] wrought Ni-based alloy and the H282-sint material reached moderate levels; however, oxidation for 5 h under steam revealed further mass gain on the H282-cast material.

In contrast, based on the kinetic data, it was found that in terms of the shape of the oxidation curves, fabrication techniques showed a significantly lower impact. The kinetic curves can be divided into three different segments. The first segment of steam oxidation, called transient oxidation, is indicated by instability during the heating period derived from the alloy composition and decomposition of different phases, nucleation, and a destabilization process upon heating and during the 1-h test. The second stage represents a protective oxide development. The third stage corresponds to volatilization of chromia scale due to the presence of dissociated hydrogen and free oxygen in the ambient atmosphere at a high temperature.

4.2 Surface

4.2.1 Surface Analyses. The surface analyses of the unexposed and the exposed materials were performed using a scanning electron microscope (SEM) in backscatter electron mode (BSE) for better characterization and identification of the phases. The surface morphologies are shown in Fig. 2(a), (b) and (c). For better traceability of changes upon high-temperature steam oxidation, the unexposed surface morphologies were added as well. The surface of the exposed alloys from the different fabrication methods showed some variations similar to the kinetic data. The phase constitutions are similar; however,

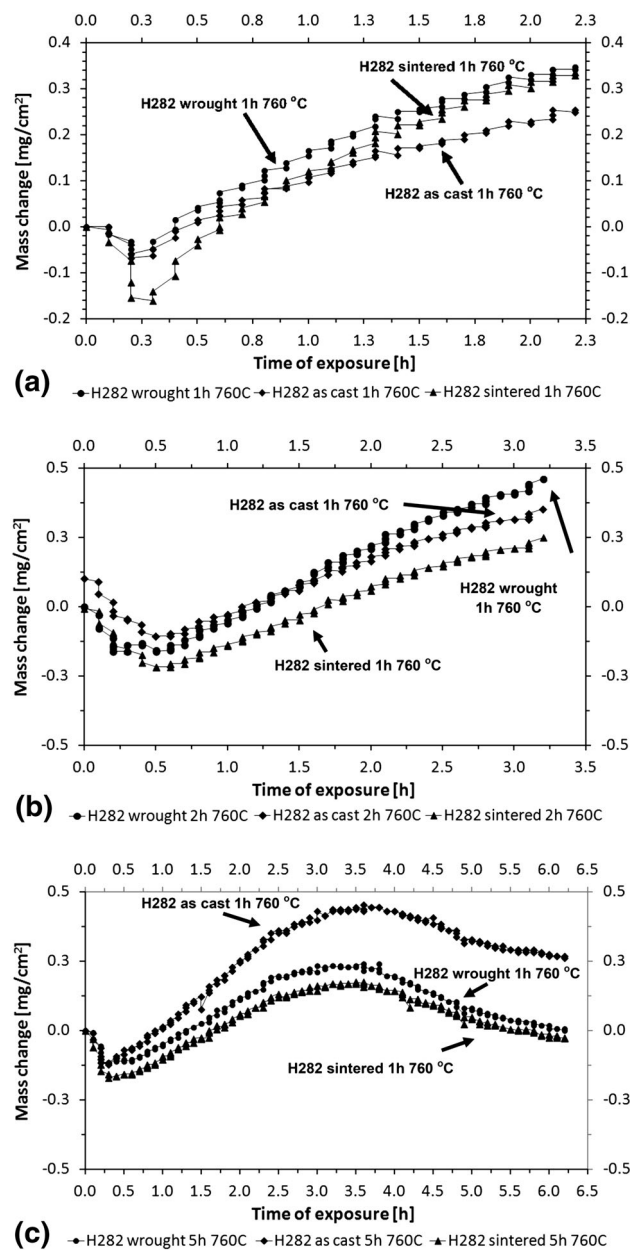


Fig. 1 Mass change data for the exposed materials in steam atmosphere after (a) 1, (b) 2 and (c) 5 h at 760 °C

composition of the formed phases varies from alloy to alloy. It has been found that exposure of the differently fabricated Haynes[®] 282[®] alloys developed two regions with different coloration, indicating different chemical compositions.

The phases formed on the exposed surface of the wrought Haynes[®] 282[®] sample are shown in Fig. 2(a); the white phase (WP) contained 18.3 wt.% of Cr, whereas the dark phase (DP)

possessed 27.9 wt.% of Cr. In contrast, Ni concentration was lower in DP (28.5 wt.%) and much higher within WP (42.6 wt.%). Contrary to the H282-cast sample, Al and Ti

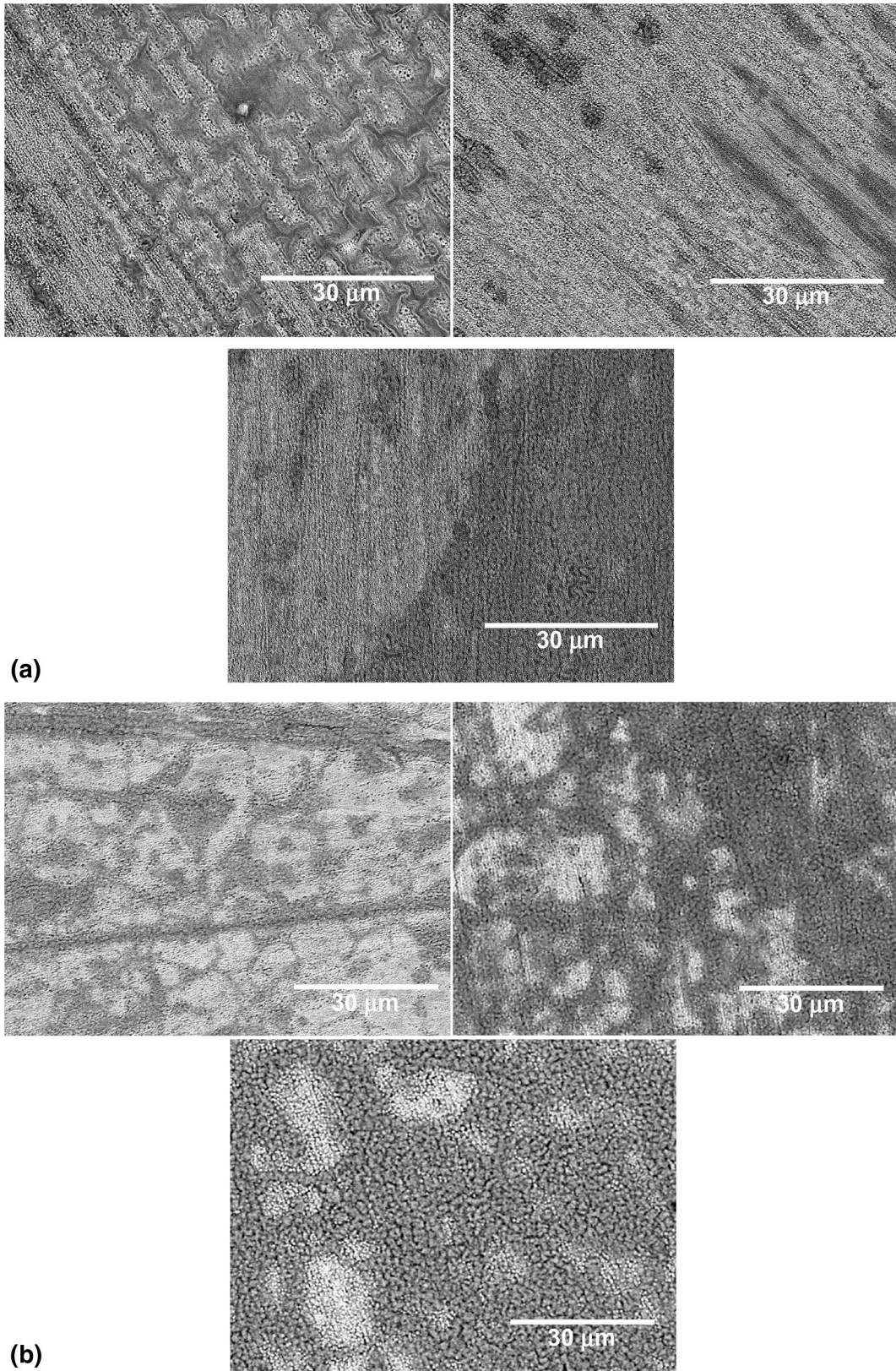


Fig. 2 Surface morphologies of the samples after steam 0 as polished), 1, 2 and 5 h of exposure at 760 °C in steam environment: (a) wrought Haynes[®] 282[®], (b) H282-cast and (c) H282-sint

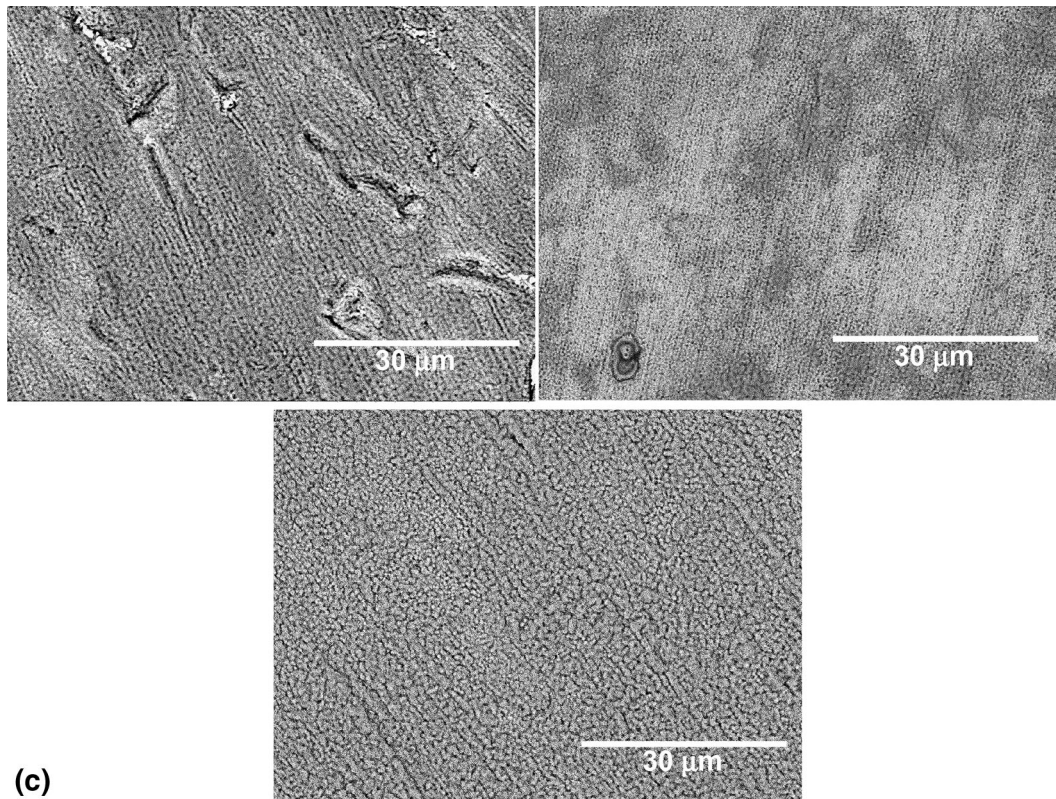


Fig. 2 continued

concentrations were always lower in WP than in DP. Furthermore, Mo concentration in DP was two times lower than that found in WP, i.e., 4.5 wt.% in DP and 9.1 wt.% in WP. Surface of the H282-cast alloy, after 1 hour of exposure, is shown in Fig. 2(b).

The exposure in steam conditions caused the formation of the white phase (WP) to have a higher concentration of Cr (21.8 wt.%) than that found in dark phase (DP) showing 19.2 wt.%. Ti concentration was lower in WP (1.7 wt.%) than in DP (2.3 wt.%). In contrast, the Al concentration in WP was higher (2.2 wt.%) than that discovered in DP (1.25 wt.%). Molybdenum concentration was similar in both phases (6.3 wt.%). Finally, the H282-sint alloy shown in Fig. 2(c), similar to H282-cast and wrought Haynes[®] 282[®] sample, showed changes within the phases. The Ni concentration in WP was much higher than that measured in DP (40.7 and 25.9 wt.%, respectively). In contrast, Cr concentration showed different behaviors; that is, more Cr was found in DP (28.2 wt.%), while in WP there was only 19.8 wt.% Cr. The analyses performed after 2 and 5 h showed similar readings, suggesting a high stability of the material under steam oxidation.

4.2.2 Cross Section Analyses. Microstructures of cross-sectioned samples characterized with high-resolution scanning electron microscopes Nova Nano and Scios Dual Beam Scanning electron (BSE) Microscope by FEI are shown in Fig. 3(a), (b) and (c). The images have been produced using the BSE detector for better contrast resolution. The observation revealed that wrought Haynes[®] 282[®], H282-cast and H282-sint alloys showed the formation of thin oxide scale with high

concentration of Cr and O suggesting the formation of Cr₂O₃ rich scale. The wrought Haynes[®] 282[®] alloy developed the oxide scale with composition of 48 wt.% Cr and 29 wt.% O, with other elements such as: Ni, Ti, Mo, Al and Co concentrated in 9.7, 6.3, 2.2 and 0.9 wt.%, respectively; however, the oxide scale demonstrated poor adhesion to the substrate (Fig. 3a). In contrast to wrought Haynes[®] 282[®] alloy, exposure of H282-cast material showed the development of empty-sphere, granular oxides on the surface (Fig. 3b) and the oxide scale had better adhesion, including a lack of spallation, voids and lateral cracks, than that shown in wrought Haynes[®] 282[®] alloy. Chemically, the composition of the oxide scale, based on EDS quantitative analyses, was as follows: 45 wt.% Cr and 25 wt.% O with addition of Ni, Co and other alloying elements. Finally, the H282-sint alloy (Fig. 3c), similar to the wrought Haynes[®] 282[®] and H282-cast alloys, presented the formation of thin oxide scale rich in Cr and O, clearly suggesting the development of Cr₂O₃-rich oxide scale. The cross-sectioned image performed by high-resolution SEM revealed the formation of voids at the interface of the oxide scale and the substrate. The presence of voids can be associated with the sintering process applied to the material. The sintered alloy shows some areas with reduced density where primary particle boundaries (PPBs) are distinguishable. These PPBs are common structural defects in sintered Ni-based superalloys (Ref 17); however, in this study there is no clear experimental evidence that PPBs influence overall performance of the alloy at high temperatures. Figure 4 to 6 show EDS x-ray mappings of the exposed alloys for better understanding of oxidation phenomena at 760 °C in steam atmosphere. The EDS x-ray

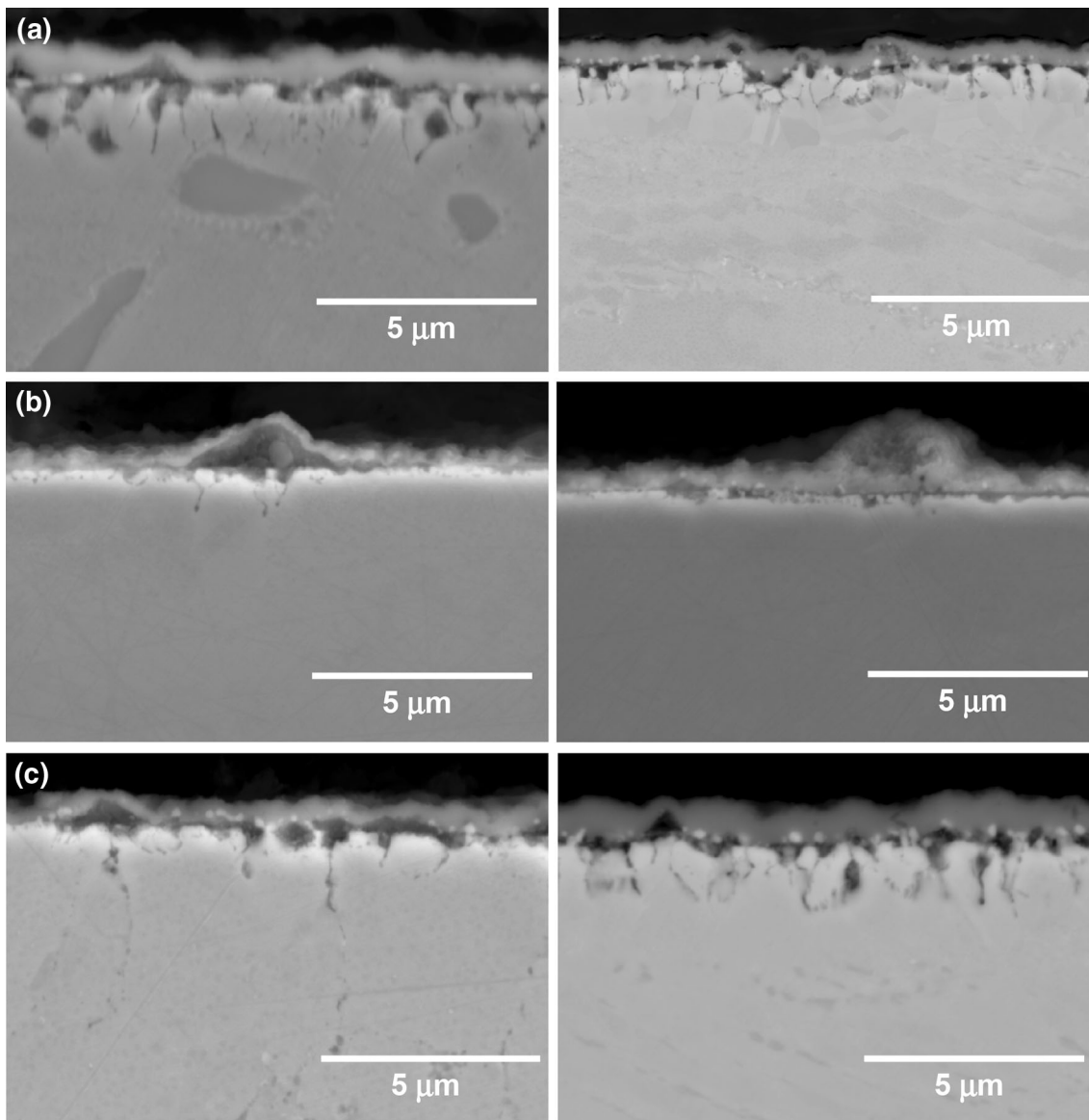


Fig. 3 Cross section microstructures in BSE mode of the exposed samples after 5 h at 760 °C in steam atmosphere: (a) Haynes® 282® wrought alloy, (b) H282-cast and (c) H282-sint

mapping of wrought Haynes® 282® carried out on the cross-sectioned sample is shown in Fig. 4 and confirmed findings from other analyses performed. For example, the oxide scale formed is primarily rich in Cr and O, with very little Ti content. Underneath the oxide scale, rich Al bandwidths were discovered. Further analyses via EDS x-ray mapping of wrought Haynes® 282® revealed that the metal matrix contained enriched areas of Ti. Figure 5 shows EDS x-ray mapping of the cross-sectioned H282-cast alloy exposed for 5 h at 760 °C in steam mixed atmosphere. Similar to wrought Haynes® 282® alloy, oxide scale formation rich in Cr and O was found. Underneath the oxide scale, a rich band of Ti and Al was also present. EDS x-ray mapping of H282-sint is shown in Fig. 6. Similar to wrought Haynes® 282®, an enriched band of Al was observed just underneath the oxide scale, consisting of Cr and O, suggesting the formation of a Cr₂O₃ rich scale. In addition, Al rich, sharp areas have been localized in grain boundaries similar to Haynes® 282® wrought alloy.

5. Discussion

The work performed in this study was initiated to investigate the influence of differing manufacturing processes on the initial stages of high-temperature steam oxidation of Haynes® 282® alloy. In this work, steam oxidation behavior of commercially wrought Haynes® 282® alloy was compared with fabricated cast alloy (H282-cast) and HIP/PM alloy (H282-sint). The alloys produced by the three different manufacturing processes were exposed to the same steam conditions at 760 °C for 1, 2 and 5 h. The importance of this research derives from the fact that the initial stages of oxidation significantly influence high-temperature corrosion performance during longer exposures. It is important to note that the exposed alloys all developed similar thin, protective, well-adherent oxide scale externally comprised mainly of Cr₂O₃ and TiO₂; however internally, in the Haynes® 282® wrought alloy and the sintered H282-sint alloy, internal precipitations on grain boundaries were found.

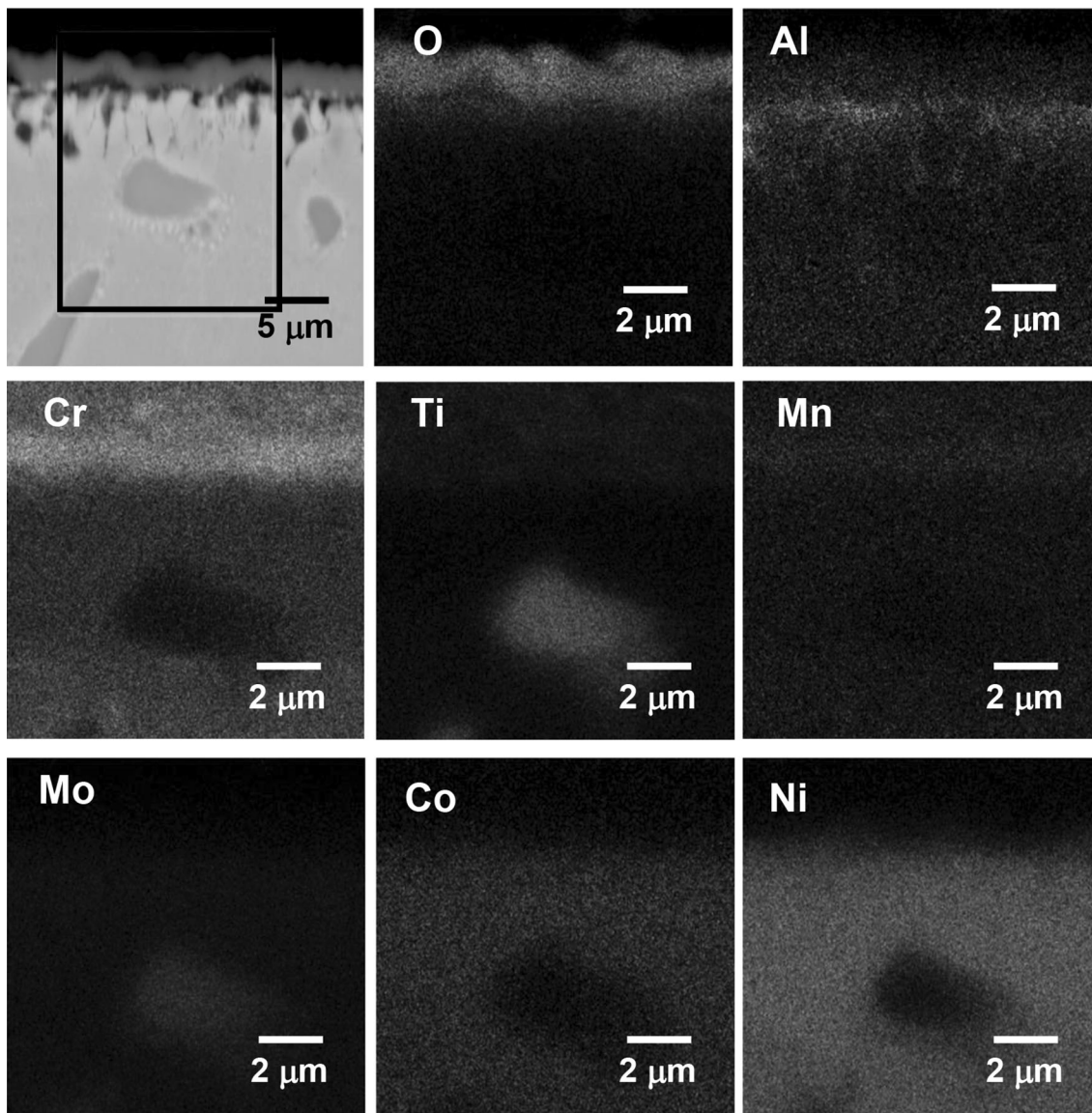


Fig. 4 EDS x-ray mapping of cross-sectioned wrought Haynes® 282® alloy exposed for 5 h at 760 °C in steam atmosphere

Therefore, this section is divided into two subsections: external scale formation and internal precipitation.

5.1 External Scale Formation

The different fabrication processes of Haynes® 282® alloy had little impact on the phase formation. All three alloys formed similar oxide scale consisting mainly of Cr_2O_3 and TiO_2 oxides. For this reason, the authors discuss the overall behavior of Haynes® 282® alloy exposed during initial steam conditions at 760 °C.

When clean, unexposed earlier nickel-based alloys containing 20 wt.% of Cr were exposed to a steam environment at high temperatures, they were expected to form oxides that would be stable under the test conditions. The stability of phases depends on activity, standard Gibbs free energy formation ΔG_7° , concentration and partial pressure of oxidizing gas, and finally diffusivity of an element. At 760 °C, when deionized water is transported from the reservoir to the hot furnace, the following reaction spontaneously occurs:



$$\Delta G_{\text{H}_2\text{O}} = 230.000 - 8.14T \cdot \ln(T) + 9.25T \quad (\text{Eq 3})$$

Further, when steam surrounds the surface of the exposed alloy, a clean surface of the alloy in rich oxidized atmosphere immediately becomes covered with oxidation by-products, leading to the formation of more stable phases such as: Al_2O_3 , Cr_2O_3 , TiO_2 . Subsequently, oxidation of an alloying element and the formation of particular oxide as mentioned above is determined by, i.e., standard Gibbs free energy formation ΔG_7° . The values in this work have been calculated based on work performed by Alcock (Ref 18). The calculated standard Gibbs free energy formation ΔG_7° in KJ/mol for Al_2O_3 , TiO_2 , Cr_2O_3 gives the -900.5 , -749.6 and -566.9 values, respectively.

The performed EDS quantitative analyses and EDS x-ray mappings confirmed only several oxides, which in this work, the authors chose to focus on; Al_2O_3 , TiO_2 and Cr_2O_3 . Activities of the elements can be calculated from well-known

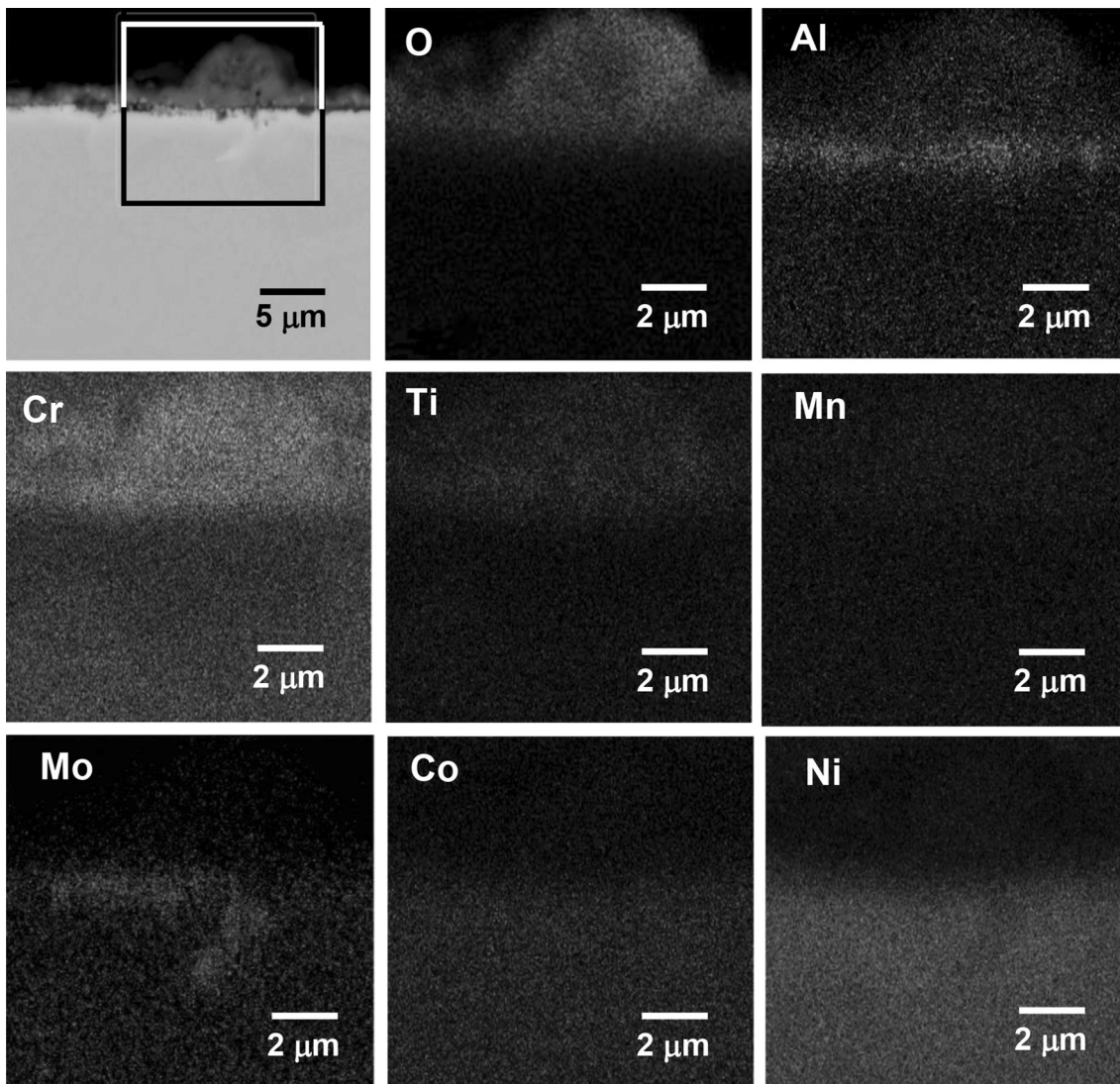


Fig. 5 EDS x-ray mapping of cross-sectioned H282-cast alloy exposed for 5 h at 760 °C in steam atmosphere

chemical reactions of the formation using the following formulas:

$$\Delta G_{\text{Al}_2\text{O}_3, T}^{\circ} = -RT \ln K_{\text{Al}_2\text{O}_3} = -RT \frac{a_{\text{Al}_2\text{O}_3}}{(a_{\text{Al}})^2 \cdot (p_{\text{O}_2})^{3/2}} \quad (\text{Eq 4})$$

$$\Delta G_{\text{TiO}_2, T}^{\circ} = -RT \ln K_{\text{TiO}_2} = -RT \frac{a_{\text{TiO}_2}}{a_{\text{Ti}} \cdot p_{\text{O}_2}} \quad (\text{Eq 5})$$

$$\Delta G_{\text{Cr}_2\text{O}_3, T}^{\circ} = -RT \ln K_{\text{Cr}_2\text{O}_3} = -RT \frac{a_{\text{Cr}_2\text{O}_3}}{(a_{\text{Cr}})^2 \cdot (p_{\text{O}_2})^{3/2}} \quad (\text{Eq 6})$$

Figure 7 shows the minimum activity graph for Ti and Cr elements where Log a versus Log p_{O_2} is present and the blue thick stripe indicates Log p_{O_2} in water steam at 760 °C according to work carried out by Dooley (Ref 19). Based on Fig. 7, it is revealed that the Ti element showed the highest activity among all of the elements present, while the Cr element showed the lowest activity. Nevertheless, at high temperature, a much higher concentration of Cr than Ti in the metal matrix causes a higher diffusion rate from the metal matrix to the surface of the alloy, resulting in enrichment of Cr on the surface

and the formation of Cr_2O_3 -rich oxide scale. The formation of Cr_2O_3 changed the balance of the activities of Ti, Cr and oxygen produced via reaction of water decomposition at high temperatures. The Cr_2O_3 formation rate decreases with time upon exposure and the formation of Ti-based oxide increases. Since concentration and activity of Ti is slightly higher than those of Al, the formation of TiO_2 is likely to form instead of Al_2O_3 on the exposed surface (confirmed by EDS x-ray mapping), and hence development of enriched areas of Ti has been found within Cr_2O_3 -rich oxide scale. Similar to the results obtained in this work, the study carried out by Cruchley et al. (Ref 20) showed that the growth rate of the chromia layer is significantly greater than that observed in Ti-free samples. The accelerated oxidation rate in Haynes[®] 282[®] according to arguments showed by Cruchley et al. (Ref 20) is attributed to increased ionic transport caused by doping of the chromia layer by titanium and creation of vacancies on the chromium sublattice. In the past, the effect of Ti in Ni-based alloys with addition of Ti has been shown by Chen et al. (Ref 21), Kim et al. (Ref 22) and recently by Taylor et al. (Ref 23). Furthermore, it has been found that Ti has a negative effect on chromia scale due to the formation of a higher number of

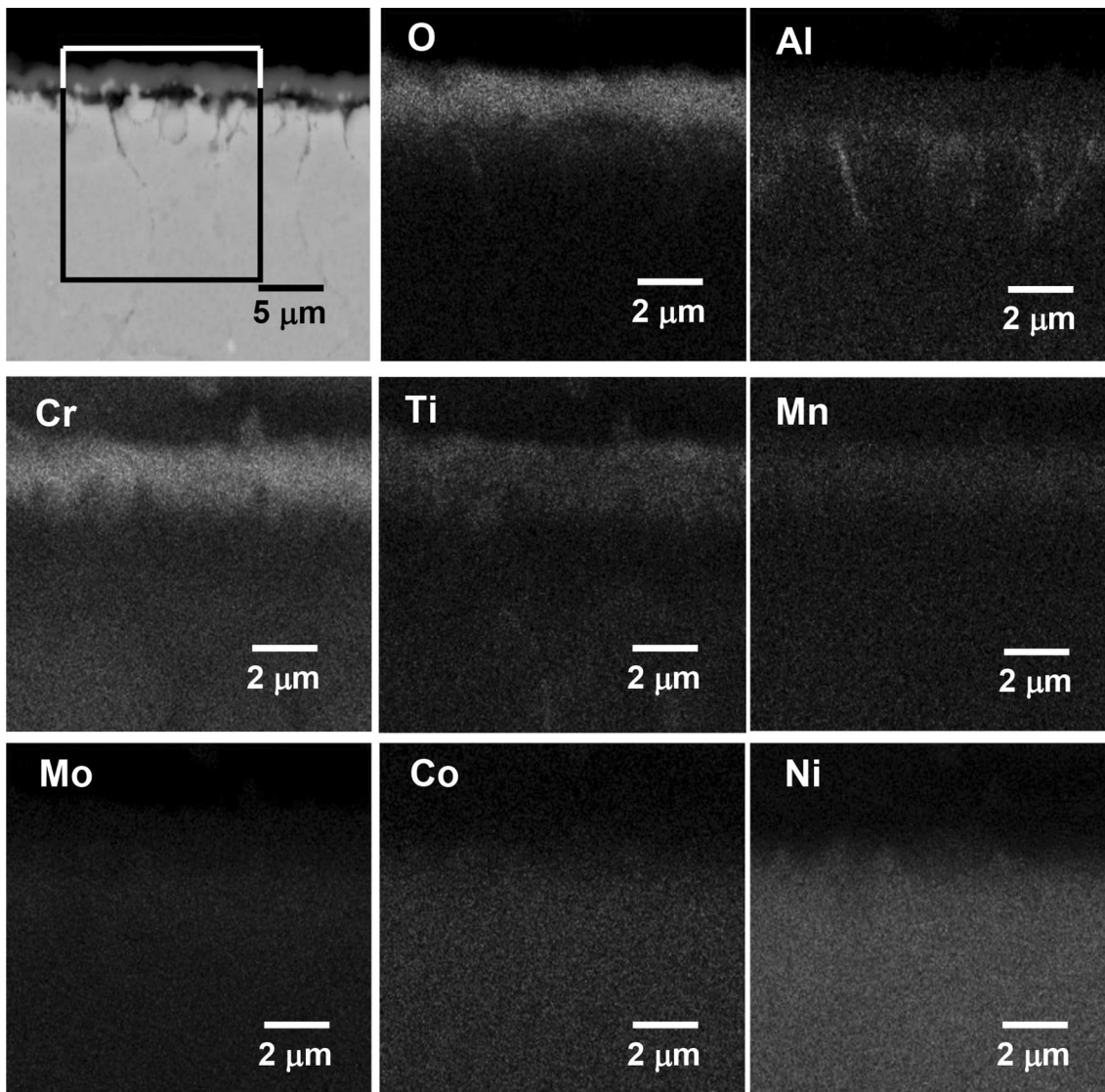


Fig. 6 EDS x-ray mapping of cross-sectioned H282-sint alloy exposed for 5 h at 760 °C in steam atmosphere

chromium vacancies, which induce directly higher diffusion rates of the chromium ion through the oxide scale. However, concentration of Ti in the chromia scale is likely to be reduced due to oxide scale thickening and depletion of Ti in the alloy.

5.2 Internal Precipitation

It has been found that two of the three alloys tested in this work, Haynes[®] 282[®] wrought alloy and sintered H282-sint alloy, underwent an internal precipitation process at 760 °C in the initial stage of steam oxidation. It is therefore possible to conclude, based on the experimental data achieved in the study, that the presence of Ti and Al in the metal matrix highly enhanced susceptibility to the internal oxidation process at high temperatures in the steam environment. The process is driven by the ability of Ti and Al to oxidize under very low partial pressures. Furthermore both elements have a strong negative standard Gibbs free energy formation ΔG_7° , which enhances oxidation under the external oxide scale. Thus, when the oxide scale consisting of mainly Cr₂O₃ with TiO₂ in Haynes[®] 282[®]

alloy is exposed in a rich oxygen environment such as water steam, underneath the oxide scale, due to high partial pressure and high activity for Al oxidation, the formation of Al₂O₃ is more than expected. Due to a low level of Ti, formation of TiO₂ shows decreased activity. Therefore, TiO₂ is unable to form internally and Al₂O₃ is mostly observed. This observation of internal oxidation of Al₂O₃ has been similarly observed in the past by many other researchers (Ref 10-12).

6. Conclusions

This work presents the results observed after the first 5 h at 760 °C of pure water steam oxidation of the Haynes[®] 282[®] alloy. The alloy used in this work was fabricated using three different methods. Initial stages of steam oxidation of highly alloyed Ni-based alloy Haynes[®] 282[®] fabricated using different manufacturing approaches revealed that kinetically, mass change in the exposed materials showed similar behavior.

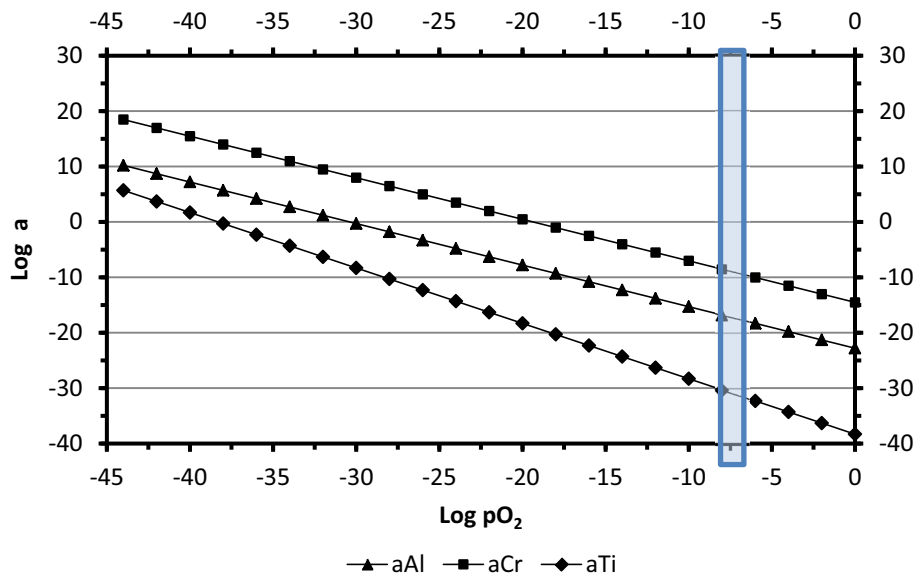


Fig. 7 Minimum activities of Ti, Al and Cr at 760 °C in steam system

Other similarities observed showed that the fabrication process strongly influences distributions of elements within the metal matrix and governs microstructures development under exposures at high temperatures in water steam conditions. Furthermore, the external oxide scale developed on the exposed alloys mainly consisted of Cr_2O_3 and TiO_2 phases. It was found that after 5 h of exposure two alloys, Haynes[®] 282[®] wrought alloy and sintered H282-sint alloy, showed development of internal precipitation zone underneath the oxide scale.

Acknowledgments

Authors like to acknowledge the support of fundamental research performed in this study to National Science Centre in Poland. Project Number: 2014/13/D/ST8/03256. The author of the work acknowledges as well materials suppliers Haynes International USA.

Open Access

This article is distributed under the terms of the Creative Commons Attribution 4.0 International License (<http://creativecommons.org/licenses/by/4.0/>), which permits unrestricted use, distribution, and reproduction in any medium, provided you give appropriate credit to the original author(s) and the source, provide a link to the Creative Commons license, and indicate if changes were made.

References

- P.J. Ennis and W.J. Quadackers, Implication of Steam Oxidation for the Service Life of High-Strength Martensitic Steel Components in High Temperature Plant, *Int. J. Press. Vessel Pip.*, 2007, **84**, p 82–87
- N. Komai, F. Masuyama, and M. Igarashi, 10-Year Experience with T23(2.25Cr-1.6 W) and T122 (12Cr-0.4Mo-2 W) in a Power Boiler, *J. Press. Vessel Technol.*, 2005, **127**, p 190–196
- J. Gabrel, C. Coussement, L. Verelst, R. Blum, Q. Chen, and C. Testani, Superheater Materials Testing for USC Boilers: Steam Side Oxidation Rate of 9 Advanced Materials in Industrial Conditions, *Mater. Sci. Forum*, 2001, **369–372**, p 931–938

- W. Quadackers, P. Ennis, J. Zurek, and M. Michalik, Steam Oxidation of Ferritic Steels—Laboratory Test Kinetic Data, Workshop on Scale Growth and Exfoliation in Steam Plant, *Mater. High Temp.*, 2005, **22**(1/2), p 47–60
- I.G. Wright, A.S. Sabau, and R. Dooley, Development of Strain in Oxides Grown in Steam. Tubes, *Mater. Sci. Forum*, 2008, **595–598**, p 387–395
- I.G. Wright, P.J. Maziasz, F.V. Ellis, T.B. Gibbons, and D.A. Woodford, Materials Issues for Turbines for Operation in Ultra-Supercritical Steam, *29th International Technical Conference on Coal Utilization and Fuel Systems*, United States, April 18-23, 2004
- S.R.J. Saunders and L.N. McCartney, Current Understanding of Steam Oxidation—Power Plant and Laboratory Experience, *Mater. Sci. Forum*, 2006, **522–523**, p 119–128
- H. Asteman, J.E. Svensson, L.G. Johansson, and M. Norell, Indication of Chromium Oxide Hydroxide Evaporation During Oxidation of 304L at 873 K in the Presence of 10% Water Vapor, *Oxid. Met.*, 1999, **52**(1/2), p 95–111
- D. Young, Effects of Water Vapour on the Oxidation of Chromia Formers, *Mater. Sci. Forum*, 2008, **595–598**, p 1189–1197
- M. Montgomery, O.H. Larsen, S.A. Jensen, and O. Biede, Field Investigation of Steamside Oxidation for TP347H, *Mater. Sci. Forum*, 2004, **461–464**, p 1007–1014
- V.P. Deodshumukh, Long-Term Performance of High-Temperature Foil Alloys in Water Vapor Containing Environment. Part I: Oxidation Behavior, *Oxid. Met.*, 2013, **79**, p 567
- I.G. Wright, Oxidation of Candidate Alloys in Steam at 17 Bar, *Final Report on Phase 1 Efforts in Support of the US Consortium Program on 'Boiler Materials for Ultra-Supercritical Coal Power Plants'*, ORNL/TM-2009/232, 2009
- N. Sobczak, Z. Pirowski, R.M. Purgert, R.W. Uhl, K. Jaśkowiec, L. Boroń, S. Pysz, J.J. Sobczak, Castability of HAYNES 282 Alloy, Workshop Advanced Ultra Supercritical Coal-Fired Power Plants, EVN Forum Maria Enzedorf Vienna, Austria, 2012
- N. Horton, R. Sheppard, Advanced Manufacturing and Materials Research for Achieving Supercritical and Ultrasupercritical Temperature Requirements, Energy Industries of Ohio at CoalGen United States, 2015
- R. Purgert, N. Horton, R. Sheppard, A Supplier Development Program for Clean Coal and Nuclear Energy Components, Energy Industries of Ohio, Final Technical Report, State of Ohio, United States, 2014
- Haynes international, High-Temperature Alloys, Technical Leaflet, United States, 2008
- P.K. Samal, Powder Metallurgy Stainless Steels: Processing, Microstructures, and Properties, Chapter 5: Sintering and Corrosion Resistance, ISBN 0871708485, 9780871708489, ASM International, 2007, p 60–100

18. C.B. Alcock, *Thermochemical Processes Principles and Models*, Butterworth-Heinemann, London, 2001
19. R.B. Dooley, Program on Technology Innovation: Oxide Growth and Exfoliation on Alloys Exposed to Steam, Technical Report, Electric Power Research Institute (EPRI) United States, 2007
20. S. Cruchley, H.E. Evans, M.P. Taylor, M.C. Hardy, and S. Stekovic, Chromia Layer Growth on a Ni-Based Superalloy: Sub-parabolic Kinetics and the Role of Titanium, *Corros. Sci.*, 2013, **75**, p 58–66
21. J. Chen, P. Rogers, and J.A. Little, Oxidation Behavior of Several Chromia-Forming Commercial Nickel-Base Superalloys, *Oxid. Met.*, 1997, **47**, p 381–410
22. D. Kim, C. Jang, and W. Ryu, Oxidation Characteristics and Oxide Layer Evolution of Alloy 617 and Haynes 230 at 900 °C and 1100 °C, *Oxid. Met.*, 2009, **71**, p 271–293
23. M.P. Taylor, H.E. Evans, S. Stekovic, and M.C. Hardy, The Oxidation Characteristics of the Ni-Based Superalloy, RR1000, at Temperatures 700–900 °C, *Mater. High Temp.*, 2012, **29**, p 145–150